

## The effect of the ring opening polymerization and chain spacing on the coefficient of thermal expansion and modulus of polyimide

Taewon Yoo,<sup>1</sup> Kwangin Kim,<sup>1</sup> Wonbong Jang,<sup>2</sup> Haksoo Han<sup>1\*</sup>

<sup>1</sup>Department of Chemical and Biomolecular Engineering, Yonsei University, 262 Seongsanno, Seodaemun-gu, Seoul 120-749, South Korea

<sup>2</sup>Department of R&D, LG Display, Gyeonggi 413-811, Korea, LG Display

Correspondence to: H. Han (E-mail: hshan@yonsei.ac.kr)

**ABSTRACT:** The features of norbornene (NE) cross-linked polyimide (PI) were investigated as the ratio of the norbornene monomer was varied. The coefficient of thermal expansion and modulus are important parameters of materials used in the microelectronic industry. Therefore, in this study, 5-norbornene-2, 3-dicarboxylic acid (NE) was introduced as a crosslinking agent to increase the thermal stability at elevated temperatures. 4,4'-Benzophenonetetracarboxylic dianhydride was utilized as a dianhydride and 4,4'-diaminodiphenyl ether was introduced as a diamine monomer. By changing the ratio of each monomer, we were able to control the spacing of the chain and ring opening polymerization, which resulted in improved properties. Each sample was thermally cured which led to a ring opening mechanism of the norbornene through the reverse Diels-Alder reaction. Thermal mechanical analysis was utilized to determine the coefficient of thermal expansion and dynamic mechanical analysis was used to determine the storage modulus ( $\epsilon'$ ) and loss modulus ( $\epsilon''$ ) of the PI film. © 2015 Wiley Periodicals, Inc. *J. Appl. Polym. Sci.* **2015**, *132*, 42607.

**KEYWORDS:** crosslinking; packaging; polyimides; ring-opening polymerization; thermal properties

Received 12 March 2015; accepted 9 June 2015

DOI: 10.1002/app.42607

### INTRODUCTION

Currently, microelectronic materials require higher performance and speed as semiconductor technology becomes more sophisticated and the distance between the vertical patterned line in the lithography process has decreased to below 20 nm.<sup>1</sup> Electronic devices are generally manufactured under extreme environments at high temperature. Therefore, materials need to endure high temperature thermal processing. The gap of the coefficient of thermal expansion (CTE) between two materials such as the substrate and coating of the polymer will cause severe quality problems such as cracking and bending of the substrate.<sup>2</sup> Therefore, it is important to understand the thermal properties of the coating materials and which factors influence them. Thermal and mechanical properties are both important in understanding the characteristics of microelectronic materials and the determination of the performance of a material.<sup>3</sup>

Among various polymers, polyimide (PI) is a well-known polymer used for coating the passivation layer of a semiconductor to protect devices.<sup>4</sup> PI contains aromatic structures, which leads to excellent thermal properties. The dominant application of PI is as a stress buffer to protect thin packages. During the curing process of PI, thermal stress is applied to the wafer which leads

to deformation, delamination, or cracking of the substrate due to the difference of the CTE values.<sup>5</sup>

Various studies have been conducted about PI synthesizing in the past.<sup>6–9</sup> Nonetheless, there is a necessity of studying about ring opening mechanism on PI to improve the thermal property. Ring opening metathesis polymerization has been used to develop new types of polymers in different fields.<sup>10</sup>

In our previous study, we have confirmed the behavior on change of dianhydrides with the property of the NE crosslinked PI.<sup>11</sup> However, the mechanism of norbornene crosslinking has not been elucidated precisely. Therefore, in this study, different ratio of norbornene was introduced as a crosslinking agent to form a three-dimensional polymer structure to enhance the thermal and mechanical properties of PI.<sup>12</sup> By changing the ratio of norbornene crosslinking in the PI structure, we were able to confirm the effect of content change of norbornene monomer on the thermal properties including the CTE and glass transition temperature.

In this study, we demonstrated that the ring opening system of norbornene is generally induced by thermal treatment during the curing process.<sup>13</sup> The complicated mechanism of ring opening polymerization takes place by the reverse Diels-Alder reaction.

**Table I.** Molar Ratio and Mass of the Norbornene Crosslinking Agents

Lot.	Diamine (ODA)	Dianhydride (BTDA)	Norbornene (NE)
(a) BONO ref	1 (1.001 g)	1 (1.611 g)	0
(b) BON(0.1)	1 (1.001 g)	0.85 (1.369 g)	0.1 (0.098 g)
(c) BON(0.3)	1 (1.001 g)	0.75 (1.208 g)	0.3 (0.294 g)
(d) BON(0.5)	1 (1.001 g)	0.65 (1.047 g)	0.5 (0.490 g)
(e) BON(0.7)	1 (1.001 g)	0.55 (0.886 g)	0.7 (0.686 g)

The structure and pathway of the norbornene end-capped crosslinking points will be elucidated in the “Experimental” section.

## EXPERIMENTAL

### Materials

For the synthesis of norbornene cross-linked PI, diamine and dianhydride monomers were purchased from Tokyo Chemical Industry, 3,3',4,4'-benzophenone tetracarboxylic dianhydride (BTDA) was introduced as the dianhydride, and 4,4'-oxydianiline (4,4'-ODA) was introduced as the diamine. 5-Norbornene-2,3-dicarboxylic and monomethyl ester (NE) was used as the crosslinking agent. The *N*-methyl-2-pyrrolidone (NMP) solvent was purchased from Duksan Chemical, Korea. All of these chemicals were used without further purification.

### Preparation of NE-Crosslinked PI Films

Specimens were prepared by changing the ratio of norbornene (NE) and the chain spacing of the polymer. Generally, PI is synthesized from polyamic acid (PAA) via diamine and dianhydride and thermally cured into PI. First, 5 mmol of 4,4'-ODA was dissolved in an aprotic dipolar solvent (NMP) for 2 h.

Second, 5 mmol of dianhydride (BTDA) was additionally dissolved in the 4,4'-ODA solution to form PAA. The mixture was stirred in an ice bath under a N<sub>2</sub> atmosphere for 12 h. N<sub>2</sub> gas was used to establish an inert atmosphere in the reactor.

Third, the norbornene monomer was added into PAA and mixed for an additional 12 h. The molar ratios of the monomers are shown in Table I and the solution of PAA contained 20 wt % of each monomer with the solvent.

Before thermal curing, the PAA was placed into a vacuum oven for 6 h to remove the micro bubbles that remain in the polymer. It is important to remove bubbles in order to prevent them from making holes in the films. The solution was generally cast at a rate of 500 rpm on a silicon wafer or glass substrate with the use of a spin coater. Before thermal curing, the substrate and coated PAA were prebaked at 80°C for 0.5 h.

The thermal curing process was automatically programmed using a regulated oven. The following steps were programmed: 100°C for 1 h, 200°C for 0.5 h, 250°C for 0.5 h, and 350°C for 2 h. The heating rate in each of the steps was 2°C/min. To reduce the residual solvents in the PI chain, it is important to utilize curing steps in the curing process. The thermal curing process is an important step to drive off solvents trapped in the

polymer structure and convert the PAA into PI by forming an imide ring.

The solvent in the PAA acts as a plasticizer and gives flexibility to the functional groups during the process.<sup>14</sup> However, in this study, our purpose was to increase the modulus of the PI by decreasing the flexibility. Therefore, eliminating the solvent from the PI is an important procedure. Furthermore, removal of the solvent helps the imide ring form in the structure. By performing a thermal curing step, we were able to reduce the amount of the solvents that were in the polymer chain. The mechanism of ring opening norbornene cross-linked PI pathway is described in Figures 1 and 2.

### Norbornene

The procedure used to synthesize NE cross-linked PI is composed of two steps. The first step is where the structure of PI is formed via poly(amic acid). Commercial PI is synthesized through a condensation reaction of diamine and dianhydride. The reaction occurs by thermal curing as the H<sub>2</sub>O is released from the monomer to form the PI. The second step starts by introducing the end capping agent which is the norbornene (NE) monomer. End capping monomers are units that terminate the reaction of a polymer chain. However, in this study, with the use of heat, the end capping monomers form network polymers.<sup>15</sup> Norbornene consists of cyclopentadiene and maleimide which break apart during the thermal curing process.<sup>16</sup> This second step allows the NE to crosslink. The critical parameters evaluated in this study were the content change of NE and the effect of the chain spacing in crosslinking on thermal and mechanical properties of PI.

## CHARACTERIZATION

### Polymer Structure

In order to characterize the change of the structure, Fourier transform infrared (FTIR, DIGILAB) spectra were evaluated to confirm the structure of the PI. The FTIR scan was conducted from 600 cm<sup>-1</sup> to 4000 cm<sup>-1</sup> with a scan speed of 2 mm/s. Samples with the size of 1 × 1 cm<sup>2</sup> were prepared for the measurements. Evaluation of the differences between the reference sample (a) BON(0), which is the PI without end-capped crosslinking, and the other NE cross-linked PI samples (b)–(e) was necessary.

### Morphology

Morphology is a key factor to determine the thermal and mechanical properties of a material. Therefore, analyzing the morphology is very crucial in polymer studies. The morphology of a polymer cannot be defined without employing X-ray diffraction (XRD) analysis as interpretation of the peaks yield information of the polymer.

Wide angle X-ray diffraction is an important instrument used to analyze the crystallinity of synthesized PI.<sup>17</sup> As the sample is irradiated with X-ray beams, the intensity of the scattered pattern is calculated and recorded. PI, which is an amorphous polymer, has partially crystalline segments in the structure. Therefore, scattering of the X-ray beam is caused by the difference of the electron density.<sup>18</sup>

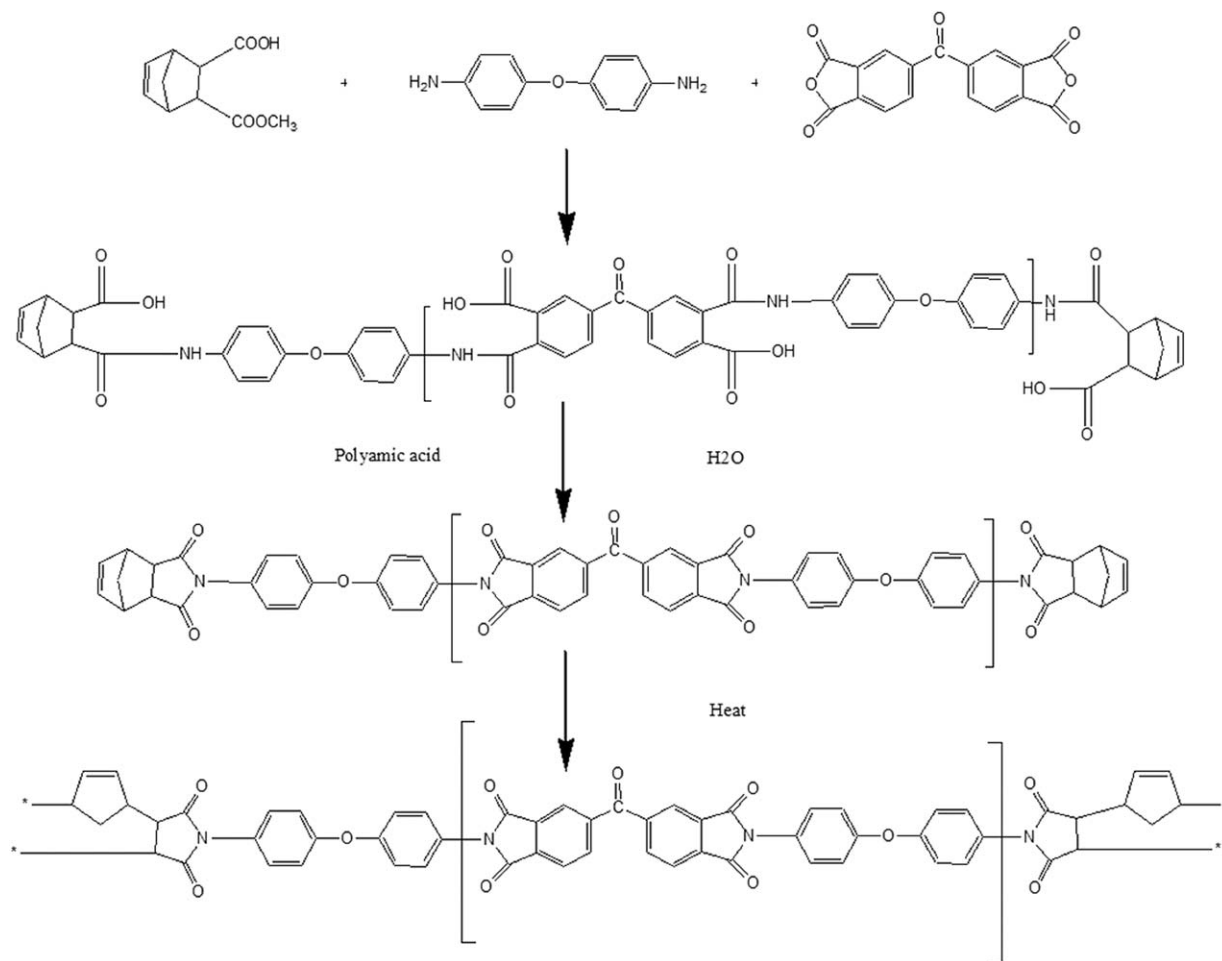


Figure 1. Pathway of NE cross-linked PI.

In this study, a Rigaku diffractometer (Model RINT 2000) was used to confirm the chain spacing between the molecules and morphology of the polymer. The XRD was operated at 40 kV/20 mA and Ni-filtered  $\text{CuK}\alpha$  was used as a radiation source. It was used with a fixed wave length of  $\lambda = 1.5405 \text{ \AA}$ . The XRD was operated in a continuous scan mode within the range of  $2\text{--}50^\circ$ . The scanning speed of the X-ray was controlled by  $2^\circ/\text{min}$ .

#### Thermal Properties

A differential scanning calorimeter (DSC) was used to detect the  $T_g$  (glass transition temperature) of the polymer. The DSC (TA Instrument, Q10) was heated from room temperature to  $400^\circ\text{C}$  at a heating rate of  $10^\circ\text{C}/\text{min}$ .

The CTE was measured by employing thermal mechanical analysis (TMA, TA Instrument, Q400). The ASTM E831 method was adapted for the process of the measurement. The instrument was heated at a heating rate of  $10^\circ\text{C}/\text{min}$  from room temperature to  $500^\circ\text{C}$  with a  $\text{N}_2$  flow rate of  $50 \text{ mL}/\text{min}$ . The end-capped PI film was prepared with a width of 4 mm and a length of 40 mm, where the thickness was controlled at  $7\text{--}8 \text{ }\mu\text{m}$ .

#### Mechanical Properties

DMA (dynamic mechanical analysis, TA Instrument, DMA Q800) was utilized using the ASTM D4065 method to measure the mechanical properties of the end-capped PI. The heating rate was  $10^\circ\text{C}/\text{min}$  from room temperature to  $500^\circ\text{C}$ . The frequency was set to 1 Hz in the tension mode.

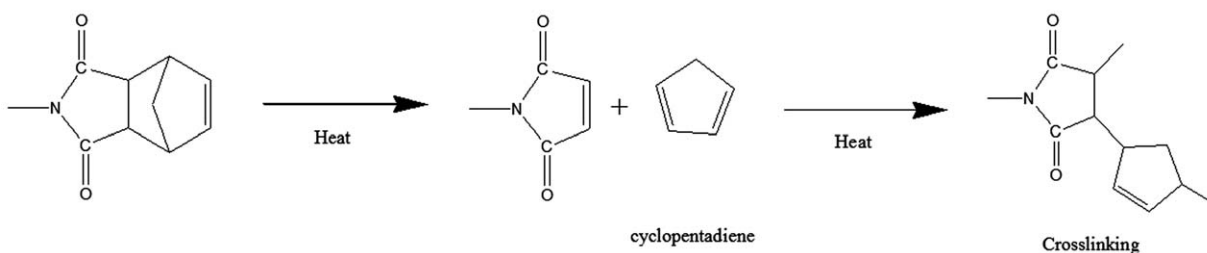


Figure 2. Ring opening mechanism of the norbornene end capper.

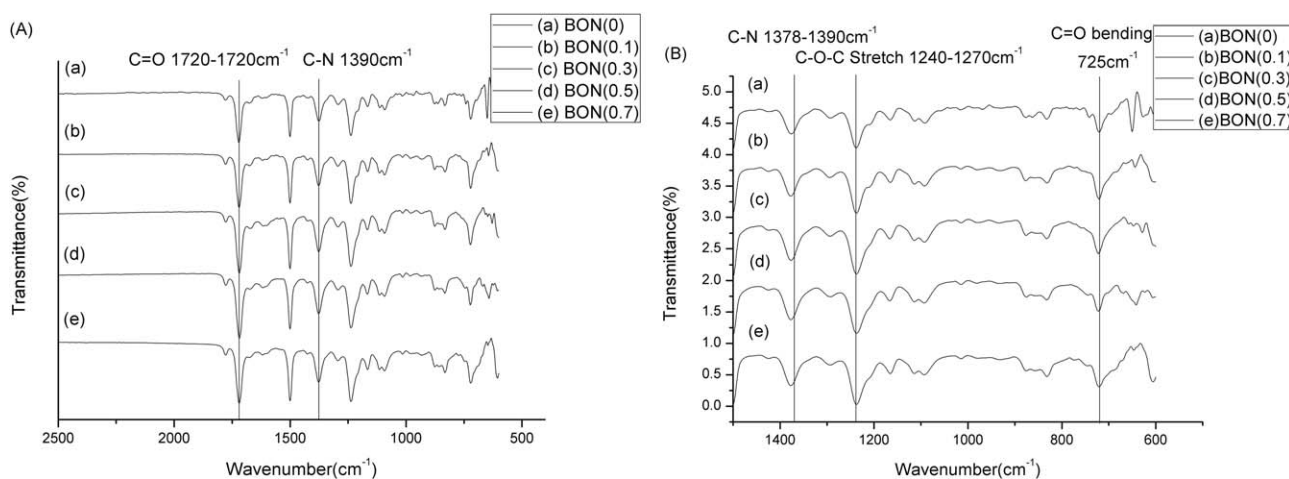


Figure 3. FTIR results of PI (A) Long range (B) Short range.

## RESULTS AND DISCUSSION

### Structure

In the FTIR spectra, we were able to confirm the structure of the polymer coating. Figure 3 shows the transmittance peaks of the norbornene cross-linked PI. C=O carbonyl stretching from carboxylic acid was observed at 1710–1720  $\text{cm}^{-1}$ .

The most crucial peaks to confirm the synthesis of PI are the  $-\text{CONH}$  peak at 1604  $\text{cm}^{-1}$  and the C–N–C peak at 1390  $\text{cm}^{-1}$ .<sup>19</sup> In a study involving curing and the structure of PI, the  $-\text{CONH}$  peak decreased as the PAA was transformed into PI.<sup>20</sup> On the other hand, as the amide group disappears, the C–N–C peak increased. The peak of C–N–C was confirmed at 1390  $\text{cm}^{-1}$ . The C=C peak at 1490  $\text{cm}^{-1}$  corresponds to stretching of the benzene ring of the PI.<sup>21</sup> The peak of NE crosslinked PI: (b)–(e), was very weak and difficult to discriminate the difference from (a)BON(0) without NE crosslinking. According to previous studies and references the peak of NE exhibited a very weak peak at 843  $\text{cm}^{-1}$  which is the crosslinking peak of C=C in norbornene.<sup>22</sup> Additionally, C–H bonds were confirmed at 810–790  $\text{cm}^{-1}$  with a very weak peak.<sup>23</sup>

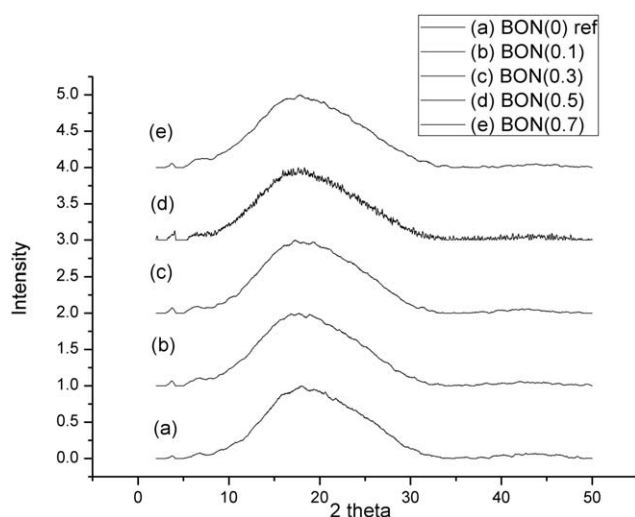


Figure 4. XRD results of PI polymers.

### Morphology

Wide angle XRD has been used for a long time to study the structure and morphology of various materials. The fraction of a polymer that is crystalline or amorphous is an important parameter to define the characteristics of the material. The features evaluated by XRD included the orientation of the structure as well as the spacing between the chain and packaging of the PI. The distance between the inter layers of PI was measured on the scale of nanometers using XRD.

The crystallinity of PI and NE cross-linked PI were evaluated by XRD. The XRD peak in Figure 4 reveals a broad peak in the region of  $20^\circ$  where  $2\theta$  is centered. From the broad XRD peaks, we can determine that the PI we synthesized is an amorphous material due to the shape of the peak.<sup>24</sup> Bragg's Law was introduced to determine the chain spacing of the NE cross-linked PI as shown below.

$$n\lambda = 2d \sin \theta$$

The equation was used to calculate the angle of diffraction of the NE cross-linked PI. The diffraction of the beam is caused by the difference of the electron density. The broad peak implies that the segments of the polymer reflected the X-ray beam and we were able to calculate the angle and chain spacing of the polymer.

In Bragg's law,  $d$  is the distance between atomic layers of a material,  $\lambda$  is the wavelength of the X-ray beams,  $n$  is an integer, and  $\theta$  is the angle between the incident ray and scattering planes.<sup>25</sup>

It is seen that  $2\sin\theta$  is proportional to  $d$  and since  $\sin\theta$  is a measure of the deviation of the diffraction from the direct beam, it is evident that structures with a large  $d$  will exhibit compressed diffraction patterns and the opposite behavior is obtained with a small  $d$ .<sup>26</sup>

Therefore, we were able to obtain the diffraction patterns and interpret the relationship between the pattern and distance among the chains. The PI properties depend on the crystallization condition and chain spacing of the polymer. The NE crosslinking played a significant role in stabilizing thermal behavior at elevated

**Table II.** Morphological Properties and Molecular Gaps between NE End-Capped PI

Polymer name	Spacing between chains	
	2theta ( $\theta$ )	Distance ( $\text{\AA}$ )
(a)BON (0) ref	18	4.93
(b)BON (0.1)	18.9	4.69
(c)BON (0.3)	19.5	4.55
(d)BON (0.5)	20.96	4.25
(e)BON (0.7)	21.08	4.23

temperatures and increasing the modulus of the material by changing the spacing between molecules. XRD is a proper instrument to determine the morphology of the polymer. From Figure 4, with the shape of the peak it was difficult to determine differences among the samples. However, by introducing Bragg's law, we were able to confirm the different chain spacing among the polymers. As shown in Table II, Sample (a) BON(0), which is PI with no crosslinking of norbornene, showed the largest chain distance of 4.93 $\text{\AA}$  which made it easier for the chains to move at elevated temperatures. As the ratio of NE crosslinking increased, we were able to observe that the spacing between the chain of (e) BON(0.7), which had the highest NE ratio, decreased to 4.23( $\text{\AA}$ ). The decrease of the chain spacing implies that the packaging of PI became more compressed in a dense state.<sup>27</sup> Dense packaging of the polymer indicates that it is difficult for the polymer chain to mobilize at elevated temperatures. Furthermore, we were able to assume that the crystallinity in the structure increased. The effect of the NE crosslinking was evaluated and the XRD analysis results were confirmed to be related to the thermal and mechanical properties.

### Thermal Properties

DSC was employed to study the thermal properties of norbornene cross-linked PI. All of the amorphous polymers exhibited a  $T_g$  during heating. Generally the glass transition temperature is the region where the hard segment of an amorphous polymer is converted to a rubbery state.<sup>28</sup> The DSC measurements performed in this study were conducted from room temperature to 400 $^{\circ}\text{C}$  under a  $\text{N}_2$  atmosphere. Endothermic peaks were observed, as shown in Figure 5.

The DSC results of NE cross-linked PI revealed that as the ratio of NE increased, the  $T_g$  consistently increased from 283.17 $^{\circ}\text{C}$  to above 400 $^{\circ}\text{C}$ . Compared to (a) BON(0), which is the reference, samples (b), (c), (d), and (e) had increased glass transition temperatures of 116 $^{\circ}\text{C}$ . This is because of the ring opening polymerization of norbornene, which caused additional crosslinking in the polymer structure.

Generally, there are two reasons for the enhanced thermal stability at elevated temperature. The first reason is that the decreased chain spacing between structures makes the mobility of the molecules difficult. This spacing result correlates with the XRD analysis. To mobilize the atoms, more heat energy is required. Therefore, the smaller the spacing, the more difficult it becomes for the chain to jiggle.<sup>29</sup> Second, additional crosslinking through the reverse Diels-Alder reaction caused the crosslinking to increase in the structure. As the NE ratio

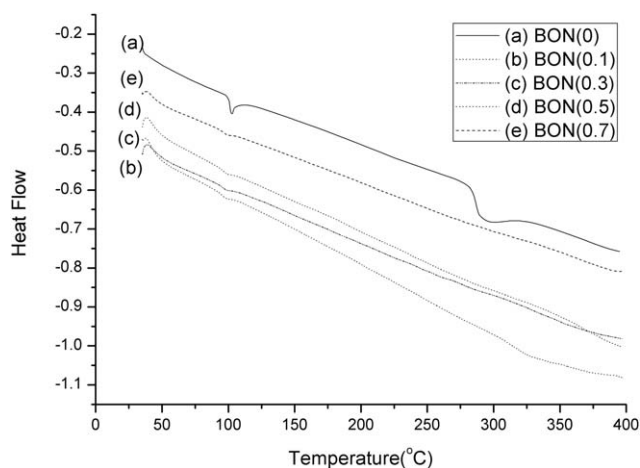
increased, the crosslinking level gradually increased through cyclopentadiene.<sup>30</sup>

The increase of NE crosslinking implies that free volume was reduced and movement is restrained of the polymer chains. This was confirmed in the DSC results and chain spacing obtained from the XRD analysis.

According to Figure 5, the first endothermic peak that is located near 100 $^{\circ}\text{C}$  is the region where  $\text{H}_2\text{O}$  evaporates from the matrix of the polymer. As the PI is heated in this region, the thermal energy of the  $\text{H}_2\text{O}$  molecules eventually becomes too large to allow the  $\text{H}_2\text{O}$  molecules to be locked into the rigid structure of the polymer. At this point, intermolecular bonds which hold the PI together are broken and reformed as the molecules move through the structure. Eventually, the thermal energy that was absorbed by the PI becomes very large such that they move too rapidly to form intermolecular bonds and the  $\text{H}_2\text{O}$  molecules start to evaporate, resulting in endothermic peaks.<sup>31</sup>

From the results obtained, (b) BON(0.1) showed a higher  $T_g$  than (a) BON(0), which is the PI sample without NE crosslinking. Moreover, (c) BON(0.3) showed a higher  $T_g$  than (b) BON(0.1) with the lowest content of NE and (e) BON(0.7) showed a higher transition temperature than (d) BON(0.5). Therefore, from these results, we can conclude that as the content of norbornene crosslinking increased, the thermal stability at high temperature increased. Generally, the PI polymer sample (a) BON(0) without NE crosslinking is loosely compressed compared to the other samples at room temperature. As the temperature was increased in the DSC experiments, the polymer absorbs heat and the bonds in the chemical structure begin to move. The molecules start to vibrate and stretch and the compression on the chain becomes loose. Therefore, the residual solvent molecules including  $\text{H}_2\text{O}$  which remained in the structure and were trapped in the chains start to evaporate as heat is absorbed. As heating continues, there is a point where the whole chain starts to move and atoms have space to show movements. The region at 283.17 $^{\circ}\text{C}$ , where the peak decreases corresponding to the absorption of heat, is the glass transition temperature ( $T_g$ ) of the (a) BON(0) sample.

$T_g$  is generally exhibited in amorphous materials such as commercial PI (a) BON(0). However, fully cured PI with NE

**Figure 5.** DSC results of NE cross-linked PI.

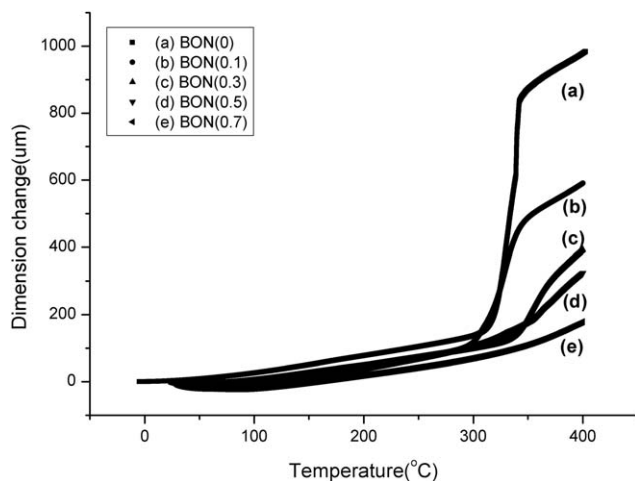


**Figure 6.** CTE of cross-linked PI with different NE crosslinking ratios.

crosslinking results in difficulty in the detection of the transition of the polymer under 400°C. Amorphous materials do not show other peaks such as the melting temperature after the  $T_g$  until the sample starts to decompose because the crosslinking prevents molecules from moving.<sup>32</sup> Given that  $T_g$  is associated with rotational freedom of the side groups of a polymer, the NE crosslinking restricted the movement of the chain segment and increased the  $T_g$ .

From the comparison of the  $T_g$  with increasing ratio of NE, it was difficult to determine the endothermic peak compared to the reference sample (a) BON(0). Therefore, DMA, which has a high sensitivity, was introduced to detect the exact transition region to characterize the thermal properties. It is difficult to distinguish the differences of the DSC results shown in Figure 5 with the analysis. The precise thermal behavior will be discussed in the DMA analysis results.

### Thermal Expansion

Reducing the difference of the CTE between the substrate and PI film and lowering it was an important consideration in this study. TMA was used to analyze the CTE of the NE cross-linked PI. Generally, the linear CTE can be expressed by the following equation.

$$\alpha_l = l/l_0 \left( \frac{\delta l}{\delta T} \right) F$$

Here,  $\alpha_l$  is the linear CTE,  $l_0$  is the original length of the sample,  $\delta l$  is the change in length,  $\delta T$  is the change of temperature, and  $F$  is the constant force applied to the sample.<sup>33</sup>

However, PI does not only expand in length, it expands in every direction.

$$\frac{\Delta V}{V_0} = \alpha_v \Delta T$$

Hence, it is important to determine the dimensional change of the polymer. Using the formula above and the TMA results, we were able to calculate the volume expansion of PI at elevated temperature. In the formula,  $\Delta V$  indicates the volume change,  $V_0$  is the original volume of the polymer, and  $\alpha_v$  is the CTE.<sup>34</sup>

In the analysis of the influence of the ratio of NE on the thermal properties using TMA, different values of the CTE were obtained. As shown in Figure 6, the CTE of the cross-linked PI was affected by the norbornene crosslinking content. As depicted in the figure, we were able to visually confirm the dimension change of (a) BON(0) which showed the largest expansion. Contrary to the (a) BON(0) sample, (e) BON(0.7) sample with the highest content of NE showed the lowest dimension change. This result is attributed to the increase of the dimensional stability due to the increase of NE crosslinking in the structure through the reverse Diels-Alder reaction, as previously described.<sup>35</sup>

The PI sample which does not contain a norbornene structure, (a) BON(0), had the highest CTE of 318.3  $\mu\text{m}/(\text{m}\cdot^\circ\text{C})$ . Table II shows the CTE values calculated using the equation above. As the amount of NE crosslinking in the PI backbone increased, the CTE decreased to 68.9  $\mu\text{m}/(\text{m}\cdot^\circ\text{C})$  for the (e) BON(0.7) sample. These CTE results are correlated with the XRD and DSC results. The expansion of the volume of PI corresponds to the  $T_g$  value. This region is the point where the transition of the polymer occurs because of different free volume in the structure.

The space that causes the transition of the PI is known as free volume. Free volume is defined as a space where a molecule has internal movement.<sup>36</sup> Due to this free volume the polymer is able to expand in the  $T_g$  region. Beyond the  $T_g$ , free volume allows space in the chain and makes more movement possible at increased temperatures.<sup>37</sup>

Hence, as the CTE values indicate, due to the additional crosslinking through the reverse Diels-Alder reaction of NE, the space between the chains decreased and resulted in low CTE values. The extended crosslinking resulted in restriction of the movement of the molecules. Thus, according to the results shown in Table III, the CTE value showed a decreasing tendency as the ratio of NE increased.

### Mechanical Properties

Dynamic mechanical data for the NE crosslinked PI series is consistent with the data that was mentioned in the “Morphology” and “Thermal Property” section.

DMA was utilized to study the temperature dependence of the storage modulus and loss modulus of the cross-linked PI. The analysis was carried out under controlled circumstances. DMA provides information about the motion changes of the chain as the temperature changes. With the use of DMA, we were able

**Table III.** Effect of the NE Content and Chain Spacing on the CTE

Polymer name	Thermal expansion measurement CTE ( $\mu\text{m}/(\text{m}\cdot^\circ\text{C})$ )
(a) BON (0)	318.3
(b) BON(0.1)	219.01
(c) BON(0.3)	148.22
(d) BON(0.5)	121.83
(e) BON(0.7)	68.9

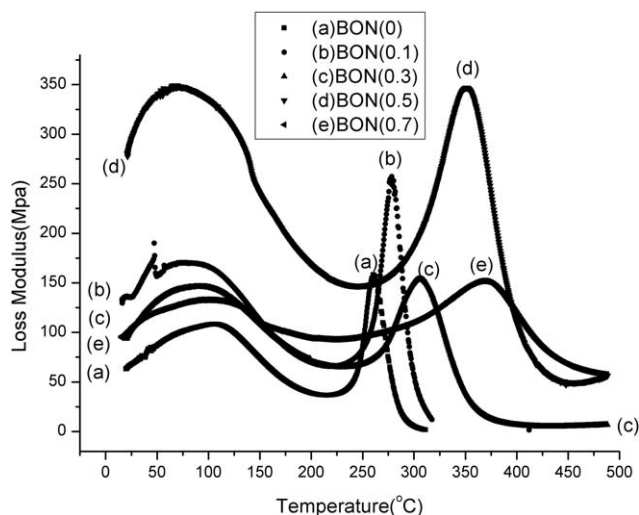


Figure 7. Loss modulus behavior as a function of the NE ratio in PI.

to measure the complex modulus ( $\epsilon^*$ ), elastic modulus ( $\epsilon'$ ), and loss modulus ( $\epsilon''$ ), which was calculated from the response of the PI sample to a sine wave.<sup>38</sup>

The elastic modulus ( $\epsilon'$ ) is generally known as storage modulus, which represents the elastic energy stored in the structure. The loss modulus ( $\epsilon''$ ) is a measure of the energy lost through heating.<sup>39</sup> The oscillation that was generally applied to the materials was fixed at 1 Hz during the measurements while the temperature was continuously changed.<sup>40</sup>

The loss modulus and storage modulus that were measured using DMA are not exactly the same as the Young's modulus and yield better characterization of the material due to the fact that we can obtain information about the loss energy ( $\epsilon''$ ), storage energy ( $\epsilon'$ ), and the ratio of the two moduli, which is the tan delta value.<sup>41</sup>

In this study, the NE monomer content was varied from 0.1 to 0.7, as discussed previously. As exhibited in Figure 7, the loss modulus of PI without NE crosslinking (a) BON(0) showed the lowest value. On the other hand, the values of the (b) BON(0.1) through (e) BON(0.7) samples showed a gradual increase proportionally due to the NE crosslinking of PI. The behavior of the polymers at elevated temperatures showed that the modulus gradually increased as the amount of NE increased. The modulus increased in the following order: (a) BON(0) < (b) BON(0.1) < (c) BON(0.3) < BON(0.5) < BON(0.7); which is in consistent with the thermal expansion and spacing between the chains.

Figure 7 illustrates the point where the loss modulus exhibits a sharp drop as the amount of NE increased in the structure of PI with less chain mobility. For each peak, the region where the modulus showed a rapid drop is the point where transition of the polymer occurs. It is the point where the glassy state of the PI is transformed into a rubbery status and loses its modulus.<sup>42</sup> The gradient of loss modulus peak increased before the  $T_g$  and decreased after it exceeded the  $T_g$  where it became a rubbery state. Loss modulus is the energy of the PI that has been dissipated as heat during the measurement. The sudden drop of the

loss modulus is the energy loss due to the decrease of friction of molecules. Above the glass transition temperature of a polymer, friction is reduced and less energy is dissipated during heating and results in decline of loss modulus. Samples (b) BON(0.1) through (e) BON(0.7) showed a gradual increase in the loss modulus where it exhibits a sharp drop as the content of norbornene increased. However, the point where the loss modulus exhibits a sharp drop of sample (e) BON(0.7) increased but the gradient before  $T_g$  decreased compared to (d) BON(0.5). The sudden drop of loss moduli of (e) BON(0.7) and (d) BON(0.5) appeared in a similar region as sample (e) BON(0.7), albeit a little bit higher.

This suggests that (e) BON(0.7) is the optimal composition to restrict movements and increase the stiffness. From this result, we can conclude that (e) BON(0.7) has the optimum content and chain spacing of NE to increase the modulus of PI. This result is attributed to the increase of crosslinking through NE. As the ratio of NE changed, the ratio of crosslinking in the PI chain increased. The reactions through norbornene crosslinking resulted in bonding with other radicals of cyclopentadiene and maleic anhydride. Derived from the crosslinking, the chain length and spacing of the molecules decreased the free volume in the structure, which correlates with the XRD data.

The crosslinking of NE introduces extended molecular chains and less spacing to the PI. Therefore, it results in more use of energy and more time to move the chain. The modulus is generally affected by the stiffness of the polymer. If the ratio of crosslinking increases in a polymer structure, the stiffness increases. Furthermore, the stiffness is affected by the free volume in the polymer. This result of the loss modulus correlates with the CTE and  $T_g$  data. We can conclude that the chain extension of the PI resulted in restriction of the movement of the sample.

A comparison of storage modulus of the PI chain with different NE ratios is displayed in Figure 8. The storage modulus is the stiffness of a viscoelastic material. The increase of the storage modulus corresponds to stiffening of the cross-linked PI backbone. The chain of the PI increased the stiffness through the ring opening mechanism of the norbornene monomer.

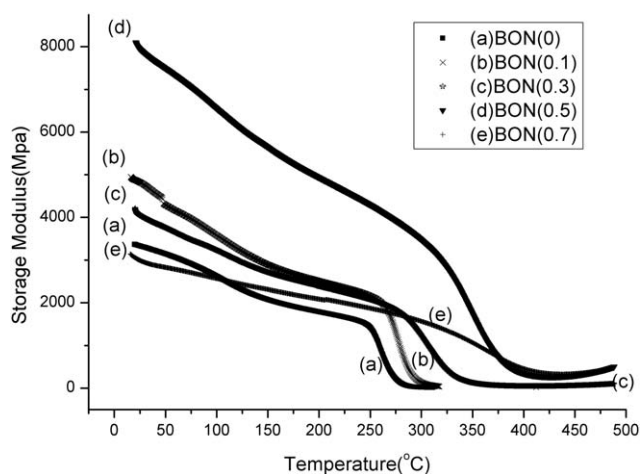
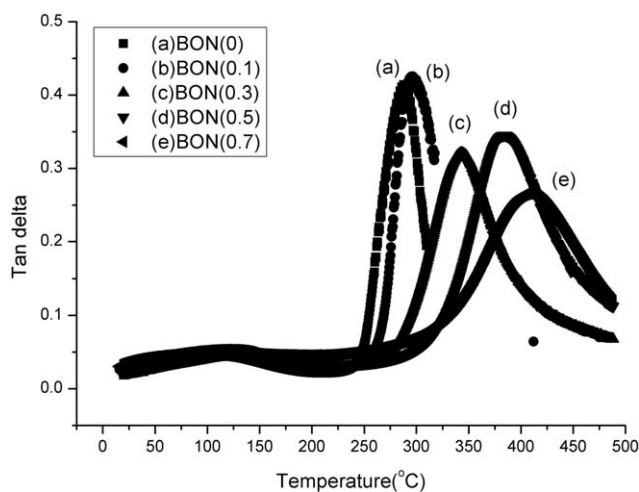


Figure 8. Storage modulus behavior of NE cross-linked PI.



**Figure 9.** Tan delta analysis results as a function of the ratio of NE obtained using DMA.

According to Figure 8, we can conclude that as the ratio of the norbornene crosslinking increased and the chain spacing declined, the storage modulus increased.

This result corresponds with the loss modulus results. Moreover, this result is related to the XRD analysis. As the NE ratio increased, the packing of the polymer became dense and the chain spacing decreased from 4.91(Å) to 4.23(Å). This fact reflects that NE crosslinking decreased the gap between the PI molecular layers. As the gap between the molecular layers decreased, the density of packaging increased which resulted in increased stiffness.<sup>43</sup>

Tan delta is the ratio of the storage modulus to the loss modulus. It is an indicator of how efficiently a material loses its energy in rearranging the polymer structure.<sup>44</sup>

$$\tan \delta = \epsilon'' / \epsilon' = \eta' / \eta''$$

From the tan delta results, we can correlate the modulus and glass transition temperature. According to Figure 9, the steep peak of the (a) BONA(0) sample showed a sharp change under 300°C, which illustrates a rapid drop of tan delta near 283°C. However, the NE cross-linked PI samples (b)–(e) showed a sudden change of the peak above 300°C, between 350 and 420°C proportionally, demonstrating that the modulus and glass transition temperature improved. These characteristics improved due to the crosslinking through the reverse Diels-Alder reaction of NE which restrained the molecular freedom of the PI.

The most severe mechanism to decrease the molecular freedom is chemical crosslinking of cyclopentadiene in the polymer chains through covalent bonds and radical reactions in the network.<sup>45</sup> Very high crosslinking densities through NE lead to increased brittleness in the PI structure. Thus, crosslinking reduced the segmental motion of the molecule at elevated temperatures.

This result of the modulus analyses is consistent to the XRD molecular spacing results. As the spacing between molecules decreased, the packaging of the chain became dense with an improved modulus. Therefore, it was difficult for the polymer to flow at elevated temperatures.

## CONCLUSIONS

The reverse Diels-Alder reaction of NE was confirmed based on the outstanding results obtained from the PI samples. The most important parameters of this study were the content of NE and the effects of the chain spacing on the property of PI. Thermal behavior along with the modulus of the NE cross-linked PI increased thermal stability remarkably. The  $T_g$  increased from 283.17°C to over 400°C. The CTE decreased from 318.3  $\mu\text{m}/(\text{m}\cdot^\circ\text{C})$  to 68.9  $\mu\text{m}/(\text{m}\cdot^\circ\text{C})$ . The wide angle XRD analysis showed that as the content of NE increased, the chain spacing of the polymer decreased, which led to dense packaging of the PI.

Increase of NE crosslinking lead to dense packaging in the structure. Therefore, the free volume of the chain decreased and resulted in low thermal expansion at elevated temperatures. Furthermore, the mechanical properties increased due to the stiffness of the crosslinking as confirmed by the DMA analysis. Consequently, as the ratio of NE increased, the thermal properties including the CTE and glass transition temperature increased thermal stability at elevated temperature and the modulus of the materials increased.

## ACKNOWLEDGMENTS

This work was supported by the National Research Foundation of Korea Grant funded by the Korean Government(MEST) (NRF-2009-C1AAA001-2009-0092926).

## REFERENCES

- Liou, H.-C.; Willecke, R.; Ho, P. S. *Thin Solid Films* **1998**, 323, 203.
- Song, G.; Zhang, X.; Wang, D.; Zhao, H.; Chen, C.; Dang, G. *Polymer* **2014**, 55, 3242.
- Chen, S. T.; Wagner, H. H. *J. Electron. Mater.* **1993**, 22, 797.
- Lee, G.; Kim, Y.; Kwon, D. *Microelectron. Eng.* **2010**, 87, 2288.
- Ji, D.; Jiang, L.; Cai, X.; Dong, H.; Meng, Q.; Tian, G.; Wu, D.; Li, J.; Hu, W. *Org. Electron.* **2013**, 14, 2528.
- Jang, W.; Shin, D.; Choi, S.; Park, S.; Han, H. *Polymer* **2007**, 48, 2130.
- Seo, J.; Han, H. *Polym. Degrad. Stab.* **2002**, 77, 477.
- Chung, H.; Lee, J.; Hwang, J.; Han, H. *Polymer* **2001**, 42, 7893.
- Jang, W.; Seo, W.; Lee, C.; Paek, S.-H.; Han, H. *J. Appl. Polym. Sci.* **2009**, 113, 976.
- Carvalho, V. P., Jr.; Ferraz, C. P.; Lima-Neto, B. S. *Eur. Polym. J.* **2012**, 48, 341.
- Kim, K.; Yoo, T.; Kim, J.; Ha, H.; Han, H. *J. Appl. Polym. Sci.* **2015**, 132, 41412.
- McClung, A. J. W.; Ruggles-Wrenn, M. B. *Polym. Test.* **2008**, 27, 908.
- Selladurai, M.; Sundararajan, P. R.; Sarojadevi, M. *Chem. Eng. J.* **2012**, 203, 333.
- Kawai, K.; Hagura, Y. *Carbohydr. Polym.* **2012**, 89, 836.
- Malcolm, P. S. *Polyimides*, In *Polymer Chemistry and Introduction*, 3rd ed.; Oxford: New York, **1999**; p 387.



16. Baugher, A. H.; Espe, M. P.; Goetz, J. M.; Schaefer, J.; Pater, R. H. *Macromolecules* **1997**, *30*, 6295.
17. Laguitton, B.; Mison, P.; Sillion, B.; Brisson, J. *Macromolecules* **1998**, *31*, 7203.
18. Suryanarayana, C.; Norton, M. G. X-Ray and diffractions, In *X-Ray Diffraction a Practical Approach*; Plenum Press: New York, **1998**; p 15.
19. Saeed, M. B.; Zhan, M.-S. *Eur. Polym. J.* **2006**, *42*, 1844.
20. Diahm, S.; Locatelli, M. L.; Lebey, T.; Malec, D. *Thin Solid Films* **2011**, *519*, 1851.
21. Shao, L.; Chung, T.-S.; Goh, S. H.; Pramoda, K. P. *J. Membr. Sci.* **2005**, *256*, 46.
22. Conreur, C.; Francillette, J.; Laupretre, P. *J. Polym. Sci. Part A: Polym. Chem.* **1997**, *35*, 123.
23. Hay, J. N.; Boyle, J. D.; Parker, S. F.; Wilson, D. *Polymer* **1989**, *30*, 1032.
24. Longun, J.; Iroh, J. O. *Carbon* **2012**, *50*, 1823.
25. Le, N. L.; Wang, Y.; Chung, T.-S. *J. Membr. Sci.* **2012**, *415*, 109.
26. Suryanarayana, C.; Norton, M. G. The structure factor, In *X-Ray Diffraction a Practical Approach*; Plenum Press: New York, **1998**; p 52.
27. Jung, Y.; Yang, Y.; Kim, S.; Kim, H.-S.; Park, T.-G.; Yoo, B. W. *Eur. Polym. J.* **2013**, *49*, 3642.
28. Rieger, J. *Polym. Test.* **2001**, *10*, 199.
29. Schneider, H. A. *Polymer* **2005**, *46*, 2230.
30. Jin, X.; Huang, L.; Shi, Y.; Yang, S.; Hu, A. *J. Anal. Appl. Pyrol.* **2002**, *64*, 395.
31. Malcolm, P. S. Molecular weight and intermolecular forces, In *Polymer Chemistry and Introduction*, 3rd ed.; Oxford: New York, **1999**; p 62.
32. Harry, R. A.; Frederick, W. L.; James, E. M. Morphology, Glass transition and polymer crystallinity, In *Contemporary Polymer Chemistry*, 3rd ed.; Pearson Education: New Jersey, p 521.
33. Wang, L.; Yu, X.; Wang, D.; Zhao, X.; Yang, D.; Urrehman, S.; Chen, C.; Zhou, H.; Dang, G. *Mater. Chem. Phys.* **2013**, *139*, 968.
34. Hevin, P. M. Experimental considerations with TMA samples, In *Dynamic Mechanical Analysis a Practical Introduction*, 2nd ed.; Taylor & Francis Group: New York, p 9.
35. Meador, M. A. B.; Johnston, J. C.; Cavano, P. J. *Macromolecules* **1997**, *30*, 515.
36. Cheng, M.-L.; Sun, Y.-M. *Polymer* **2009**, *50*, 5298.
37. Hevin, P. M. Expansion and CTE, In *Dynamic Mechanical Analysis a Practical Introduction*, 2nd ed.; Taylor & Francis Group: New York, p 61.
38. Shao, Q.; Lee-Sullivan, P. *Polym. Test.* **2000**, *19*, 239.
39. Sawpan, M. A.; Holdsworth, P. G.; Renshaw, P. *Mater. Des.* **2012**, *42*, 272.
40. Lee-Sullivan, P.; Dykeman, D. *Polym. Test.* **2000**, *19*, 155.
41. Faria, R.; Duncan, J. C.; Breerton, R. G. *Polym. Test.* **2007**, *26*, 402.
42. Hevin, P. M. Calculating various dynamic properties, In *Dynamic Mechanical Analysis a Practical Introduction*, 2nd ed.; Taylor & Francis Group: New York, p 75.
43. Numata, S.; Fujisaki, K.; Kinjo, N. *Polymer* **1987**, *28*, 2282.
44. Torrecillas, R.; Regnier, N.; Mortaigne, B. *Polym. Degrad. Stab.* **1996**, *51*, 307.
45. Malcolm, P. S. Chemical crosslinking, In *Polymer Chemistry and Introduction*, 3rd ed.; Oxford: New York, **1999**; p 85.